Jin, S., Liu, Y., Deiseroth, M., Liu, J., Backus, E. H. G., Li, H., et al. (2020). Use of Ion Exchange To Regulate the Heterogeneous Ice Nucleation Efficiency of Mica. Journal of the American Chemical Society, 142(42), 17956-17965. doi:10.1021/jacs.0c00920.

Use of Ion Exchange To Regulate the Heterogeneous Ice Nucleation Efficiency of Mica

Ion Exchange to Regulate Heterogeneous Ice Nucleation Efficiency of Mica

Shenglin Jin‡[a], Yuan Liu‡[b,d], Malte Deiseroth‡[c], Jie Liu†[a], Ellen H.G. Backus[c,f], Hui Li[b], Han Xue[a], Lishan Zhao[a], Xiao Cheng Zeng*[d], Mischa Bonn*[c], Jianjun Wang*[a,e].

[a]*Key Laboratory of Green Printing, Beijing National Laboratory for Molecular Science, Institute of Chemistry, Chinese Academy of Sciences, Beijing 100190, China.*

[b]*Beijing Advanced Innovation Center for Soft Matter Science and Engineering, Beijing University of Chemical Technology, Beijing 100029, China.*

[c]*Max Planck Institute for Polymer Research, 55128 Mainz, Germany.*

[d]*Department of Chemistry, University of Nebraska-Lincoln, NE 68588, USA.*

[e]*School of Chemistry and Chemical Engineering, University of Chinese Academy of Sciences, Beijing 100049, China.*

[f]*Department of Physical Chemistry, University of Vienna, Währinger Straße 42, 1090 Wien, Austria*

KEYWORDS: Ion exchange, Heterogeneous ice nucleation, Mica, Vibrational sum-frequency generation spectroscopy, Molecular dynamics simulations.

ABSTRACT: Heterogeneous ice nucleation (HIN) triggered by mineral surfaces typically exposed to various ions can have a significant impact on the regional atmosphere and climate. However, the dependence of HIN on the nature of the mineral surface ions is still largely unexplored due to the complexity of mineral surfaces. By taking advantage of the unique property that the K^+ on the atomically flat (001) surface of mica can be facilely replaced by different cations through ion exchange, muscovite mica was selected as its simpler nature provides a much more straightforward system to serve as the model for investigating the effects of mineral surface ions on HIN. Our experiments show that the surface (001) of H^+-exchanged mica displays markedly higher HIN efficiencies than that of Na-/K-mica. Vibrational sum-frequency generation spectroscopy reveals that the H-mica induces substantially less orientation ordering, compared to the Na-/K-mica, within the contact water layer at the interface. Molecular dynamics simulations suggest that the HIN efficiency of mica depends on the positional arrangement and pointing orientation of the interfacial water. Formation of the hexagonal ice I*h* basal-type structure in the first water layer atop the mica surface facilitates HIN, which is determined by the size of the protruding ions atop the mica surface and by the surface adsorption energy. The orientational distribution is optimal for HIN when 25% of the water molecules in the first water layer atop the mica surface have one OH group pointing up, and 25% have one pointing down, which, in turn, is determined by the surface charge distribution.

Introduction

Heterogeneous ice nucleation (HIN) is widely observed in a variety of environmental and biological processes. A better understanding of the mechanisms underlying HIN is of importance, for example, to the development of improved model of cloud formation, which can directly affect numerous atmospheric processes such as precipitation, radiative budget and climate on Earth.[1-5] However, predicting and tuning HIN is still very challenging nowadays, due in part to the lack of molecular-level mechanisms of HIN.[6,7] In the upper troposphere, ice particles can form in pre-existing liquid aerosols *via* homogeneous ice nucleation. As a quantitative measure, Koop *et al*. introduced water activity (*i.e.*, the ratio between the water vapor pressure of the solution and that of pure water under the same conditions) as a determinant for homogeneous ice nucleation in aqueous solution.[8]

However, ice nucleation often occurs *via* HIN on foreign surfaces in nature.[9] For instance, the surfaces of mineral dust embedded with various types of ions are key to the formation of ice clouds.[2,3,10-13] Through studying a variety of solutes together with general types of ice nucleating particles (silver iodide and silica etc.), Zobrist *et al* revealed that HIN can also be properly described by water activity only if the surface properties of the ice nucleating particles are not affected by ionic solutes.[3,13] Meanwhile, Kumar and coworkers found deviations of HIN temperatures existed with those predicted by water activity due to specific chemical interactions between particular ions in aqueous solutions and surfaces of feldspars (*i.e.*, surface ion exchange, adsorption and surface degradation).[3,10] That is, the HIN efficiency of mineral dusts differs greatly as the alteration of surface properties caused by the addition of ionic solutes.[3] Therefore, studies have been devoted to the effects of ions on ice nucleation atop a variety of mineral particles. [3,10-12,14-27] However, conflicting conclusions still exist due to the chemical and physical complexity of the mineral surfaces.[2,3,10,14,28] As such, investigation of ice

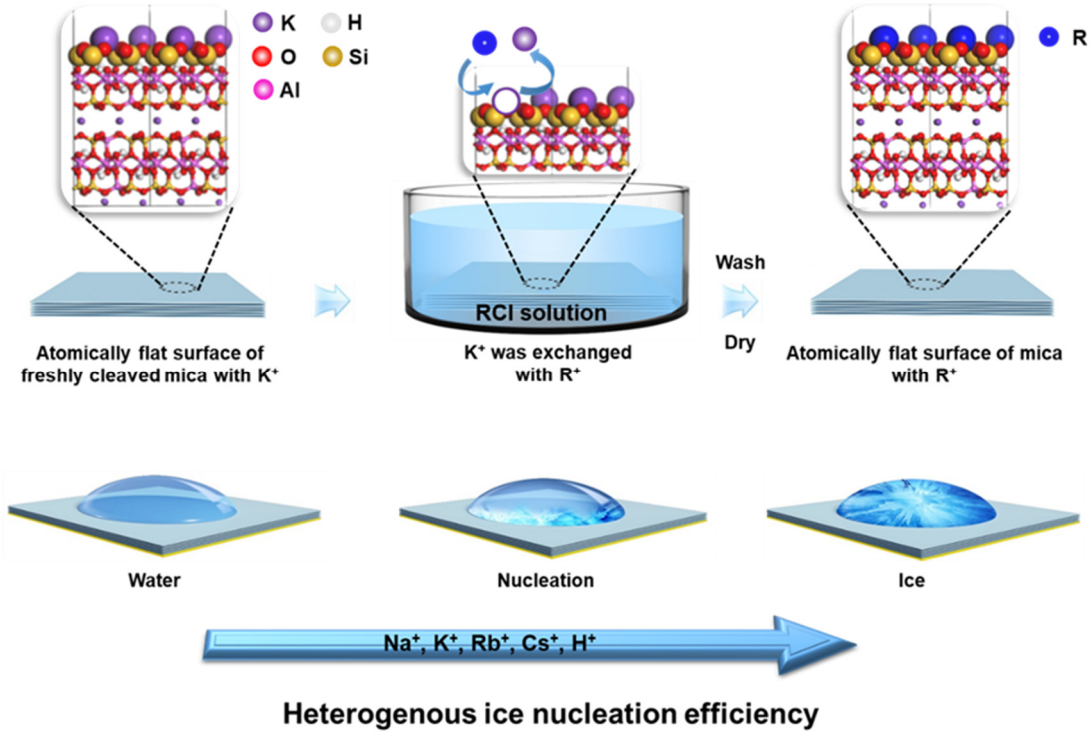

Figure 1. **Schematic illustration of HIN efficiency on mica surfaces with different cations**. The K^+ on freshly cleaved mica surfaces can be successfully exchanged to become R^+ ($R^+ \in \{Na^+, K^+, Rb^+, Cs^+ \text{ or } H^+\}$), by immersing the freshly cleaved mica into 0.5 M RCl solutions (Top panels include the expanded side view of the molecular structure of muscovite mica obtained from MD simulation slab. Purple, white, red, yellowish, pink, and blue spheres stand for potassium, hydrogen, oxygen, silicon, aluminum, and R atom, respectively.) Next, the modified mica surfaces were washed with Milli-Q water and dried with nitrogen gas. A water droplet (0.1 μL) was subsequently placed on the prepared mica surface (bottom panels). $\boldsymbol{T}_H$ was then measured in a closed cell placed on a cryostage by monitoring the nucleation of water droplets with a high-speed camera coupled with an optical microscope (**SI**).

nucleation on well-defined systems of mineral surfaces with ions is highly desired.

On the other hand, although very few theoretical and experimental studies on how the ion specificity and associated interfacial water regulate HIN, the effects of the property of interfacial water on HIN have been studied by molecular dynamics (MD) simulations.[29-35] Lupi *et al.*[29] have shown, using MD simulations, that HIN on graphitic surfaces is closely correlated with the layering of the liquid water at the interface.[29,30] This conclusion is compatible with those drawn from simulation studies of HIN on crystalline surfaces[31], on atomically flat surfaces and on surfaces with concave wedges.[34] While the role of interfacial water has been intensely studied, direct experimental studies of the effect of ions on interfacial water and on the HIN efficiency are crucial to achieving improved mechanistic understanding and tuning of HIN. In view of those, muscovite mica surfaces with different cations were undertaken in order to establish a close correlation between the ion specificity and interfacial water, and the impact of ion specificity on HIN. As mica can be freshly cleaved to have an atomically flat surface (001)[36-38], the effects of common ions[39], surface roughness, and fluctuations induced by organic surfaces[40,41] on the interaction of water/ice with the surfaces can be neglected. More importantly, when the freshly cleaved mica is immersed in aqueous solution under ambient conditions, the cation K^+ on the outmost mica surface can be readily exchanged with other cations in the solution, such as: H^+, Cs^+, Rb^+, Ca^{2+} and Na^+ depending on the concentration of ions.[42-44] Therefore, mica surfaces with varying cations can be employed as a more straightforward system for understanding the fundamental mechanisms of HIN by ions on mineral surfaces. Our measurements show that the HIN efficiency, measured by ice nucleation temperature $\boldsymbol{T}_H$ and ice nucleation delay time t_D is sensitively dependent on the cations on the mica surface. The mica surface with atop H^+-exchanged (H-mica) displays the highest HIN efficiency, while mica surface with atop Na^+ (Na-mica) has the lowest efficiency in promoting ice nucleation among mica surfaces with various cations. Vibrational sum-frequency generation (VSFG) spectroscopy analysis reveals that the H-mica has the least orientated interfacial water. In contrast, the Na-mica has the most orientated interfacial water. Moreover, MD simulations show that the smaller dipole projection along the z-direction (the surface normal direction) of the interfacial water tends to give higher freezing temperatures. The HIN efficiency of the mica surface also depends on the positional arrangement and the pointing orientation of the interfacial water.

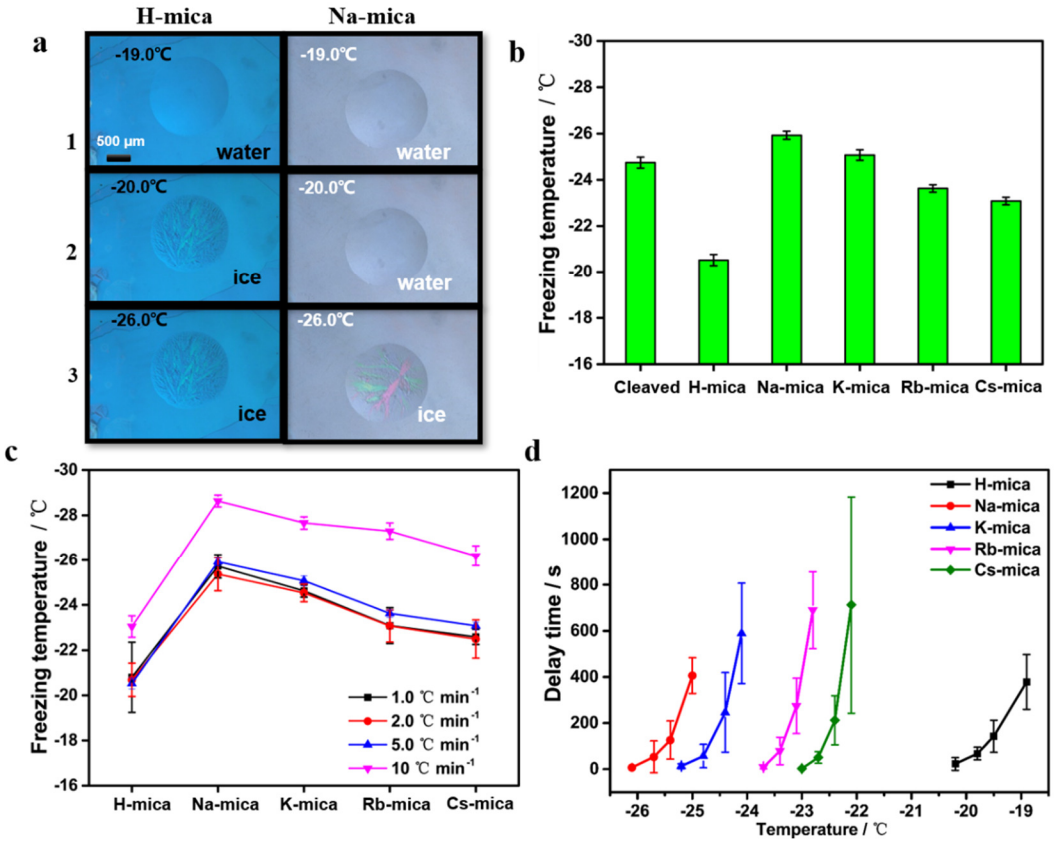

Figure 2. (**a 1-3**) A typical freezing process of a water droplet in a closed cell, *i.e.*, microscopic images of water droplet before and after freezing on the H-mica and Na-mica (001). (**b**) Ion-specific effect on the T_H of the water droplet on the surfaces (001) of cleaved mica, H-mica, Na-mica, K-mica, Rb-mica and Cs-mica. (**c**) The influence of cooling rate on T_H. (**d**) The delay time (t_D) dependence of ice nucleation on the various cation-embedded mica surfaces, which was measured by recording the time needed for ice nucleation to occur on a cation-embedded mica surface.

Results and Discussion

Effect of mica surface cations on the HIN efficiency. As shown in **Figure 1**, the expanded side view of the molecular structure of muscovite mica indicates two layers of tetrahedral SiO_4 sheets sandwiching one octahedral aluminum layer. The substitution of Si^{4+} by Al^{3+} in the SiO_4 sheet leads to intrinsic negative charges of mica surfaces, which are neutralized by electrostatically bound interlayer K^+ (the top panels of **Figure 1**).[38] This allows muscovite to be cleaved along its basal plane (001) with the K^+ distributed equally on the two freshly cleaved atomically flat surfaces.[36,37] The mica was peeled off with the entire wafer to avoid defects, and then nitrogen gas was blown gently over the exposed mica surface to remove any possible small residues. The K^+ can be exchanged by immersing the freshly cleaved mica surface into corresponding ionic solutions to obtain the mica surfaces atop with either H^+, Na^+, K^+ (K-mica), Rb^+ (Rb-mica) or Cs^+ (Cs-mica), [42,43,45] as illustrated in **Figure 1** (for more details, see Supporting Information, **SI**). **Figures S1-S2** show XPS spectra of mica surfaces after exposure to various ionic solutions. **Figure S1b** shows the appearance of the peaks in the energy region of 1080-1060 eV, 310-290 eV, 250-230 eV and 740-720 eV, indicative of Na 1s, K 2p, Rb 3p and Cs 3d orbital binding energy region, respectively. The XPS spectra confirm the success in exchanging of Na^+, K^+, Rb^+, and Cs^+ on the mica surface. The removal of Cl^- by rinsing the mica surfaces with Milli-Q water was also confirmed by XPS, due to the absence of signal in the region of Cl 2p orbital (**Figure S2**). The surface morphology and roughness of freshly prepared mica surfaces with various cations were detected by Atomic Force Microscope (AFM). As shown in **Figure S3**, no obvious difference in the morphology of the samples was identified, and the roughness of various cation-exchanged mica surface are all less than 0.8 nm. The contact angles of 0.1 uL water on various cation-embedded mica surfaces are around 8.0～10 ° , suggesting that the contact area of 0.1 uL water on mica surfaces with various cations is indistinguishable, within error (**Figure S4**). Therefore, we can safely conclude that the roughness and contact area do not affect HIN on cation-exchanged mica surface.

After drying the mica surface with flushing nitrogen gas, the T_H of water droplets (0.1 μL) on mica surfaces was measured in a closed cell[46] with different locations, and each with one freezing cycle,[47,48] and the freezing of droplets was monitored with a high-speed camera connected to an optical microscope[49] (**Figure 1**, **Figure S5** and **Scheme S1**). As shown in **Figure 2a** (**1-3**), the ice nucleation temperature T_H of water droplets on the surface of H-mica is *ca.* -20.0 °C, whereas it is *ca.*-26.0 °C on Na-mica. The order of T_H on the mica surfaces with cations is $T_{H\ H\text{-}mica} > T_{H\ Cs\text{-}mica} > T_{H\ Rb\text{-}mica} > T_{H\ K\text{-}mica} > T_{H\ Na\text{-}mica}$, as shown in **Figure 2b**, at a cooling rate of 5.0 °C min^{-1}. The mica surface with H^+ exhibits a substantially higher average T_H than those

with other alkali cations, regardless of the cooling rate as indicated in **Figure 2c**. These results unambiguously show that the T_H depends on the type of cation on the mica surfaces.

Moreover, the corresponding ice nucleation delay time (t_D) of water droplets on the surfaces of various cation-embedded mica was investigated to further validate the HIN efficiency of mica surfaces with H or alkali metal species.[50,51] The time needed (t_D, the time interval between the time when the substrate reaches a target temperature and the time when the ice nucleus appears) for the ice nucleation to occur from the water droplets was measured for each type of cation-embedded mica surface. We plot the delay time versus the temperatures, as shown in **Figure 2d**; the delay time increases exponentially as the surface temperature increases on the various cation-exchanged surfaces.[52] Moreover, by fixing three specific supercooling temperatures of -20.0 °C, -23.0 °C and -25.0 °C as shown in **Figure S6**, t_D of water droplets on the surfaces of H-, Na- and Rb-mica was further measured. At the supercooling temperature of -23.0 °C, ice nucleation occurred on the surfaces of H-, Na- and Rb-mica at about 0 s (*i.e.*, the HIN occurs before the substrate reaches the target temperature), 284 s and 3921 s, respectively. t_D on the Na-mica is nearly one and four orders of magnitude longer than that on the Rb- and H-mica, respectively (**Figure S6**). In general, t_D decreases as the supercooling temperature decreases, whereas the ice nucleation often occurs before the substrates reach the target supercooling temperature on the H-mica at -23.0 °C and -25.0 °C (**Figure S6**). Furthermore, the ice nucleation on the Na-mica requires a substantially longer average t_D than those on the H-mica and Rb-mica as shown in **Figure S6**. These results demonstrate that the H-mica markedly enhances the HIN efficiency, whereas the HIN efficiency is much lower on the Na-mica. However, the molecular mechanism causing these differences in HIN efficiency remains unclear.

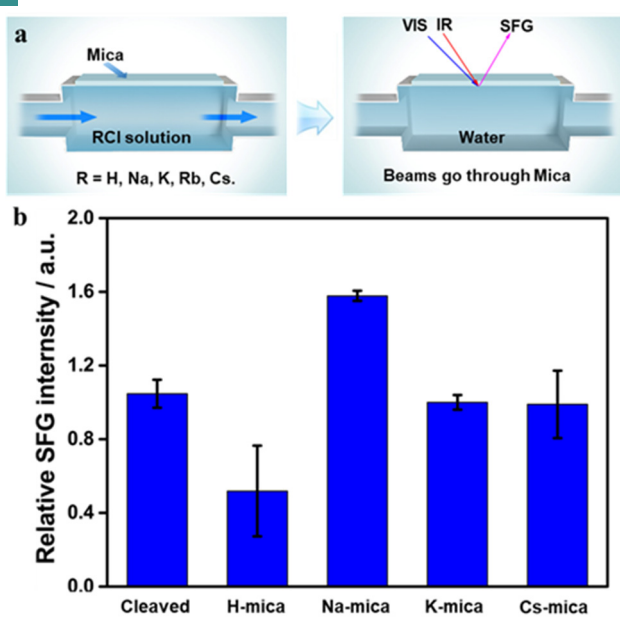

Figure 3. (**a**) A schematic illustration of the flow cell used for the measurement of SFG signals from the mica-water interface. The laser beams pass through the mica sample and overlap on the mica-water interface both in space and time. (**b**) Average SFG intensity of mica-water interfaces in the region of OH-stretch region between 3000 and 3550 cm^{-1}, which is normalized to the intensity of the K-mica-water interface (*i.e.*, an intensity of 1 per definition).

Structure of interfacial water. To investigate how the interfacial water atop mica was regulated by the surface properties, VSFG was employed. Owing to its spectroscopic selection rules, VSFG is interface specific and provides cation-specific vibrational spectra of interfacial water atop mica surfaces in the liquid state.[53] To avoid signal variations caused by sample-to-sample differences (**Figure S7**), a flow cell was used to exchange surface cations by flowing ionic solutions through the cell (**Figure 3a** and **SI**). To probe the mica-water interface, the laser beams passed through the mica sample and overlapped at the mica-water interface both in space and time. **Figure S8** shows an IR transmission spectrum of a mica sheet with a constant transmittance of about 80% through the investigated frequency region of 3000 cm^{-1} to 3550 cm^{-1}. The disappearance of SF response upon isotopic exchange of H_2O with D_2O (spectra in **Figure S9**) confirms that the observed signal originates from the mica-water, but not from the mica-air interface.

The integrated SFG intensity normalized to the intensity of the K-mica-water interface is shown in **Figure 3b** (**Figure S7**). On H-mica the integrated SFG intensity throughout the frequency range of the OH-stretch vibration is the lowest. In contrast, the integrated SFG intensity is the highest on Na-mica. As the SFG intensity correlates with the z-projection of the average water dipole moment, this means that the change of average water alignment depends on the specific cation species on the mica surface. The observed SFG intensity variations thus reflect changes in the average orientation of interfacial water dipole moments.[53] As such, the highest $\boldsymbol{T}_H$ for H-mica correlates with the lowest extent of orientation of the interfacial water. On the other hand, the Na-mica that gives the lowest $\boldsymbol{T}_H$ shows the greatest extent of orientation of the interfacial water. As a result, we conclude that the formation of ice is probably hindered by strongly oriented (Na-mica) and favored by weakly oriented (H-mica) interfacial water. This conclusion is consistent with previous reports that the density and orientation of the interfacial water govern the HIN efficiency, which can be affected by the surface lattice and/or surface charges etc.[54-57] However, this effect cannot fully explain the observed ion specific ice nucleation capability on the mica surfaces with different cations, as no clear connection has been made between the positioning and alignment of the interfacial water molecules; further, it remains to be unveiled on the relationship between the properties of interfacial water and surface cations as well as the correlation between the properties of interfacial water and the capability of HIN of mica surfaces.

Molecular-level insight into HIN on mica surfaces. To gain molecular-level insight into HIN on mica surfaces with different cations, as well as the orientation of the interfacial water atop mica surfaces, the dipole moments of water atop mica were analyzed based on the MD simulations by using both TIP6P[58] and TIP4P/Ice[59] water potentials according to the computational details in **SI**, in which water molecules within the interfacial region of 2.0 nm on the mica surface were selected (**Figure S11a**). The dipole projection along the *z*-direction (the normal direction of the surface) was used as a quantitative measurement of overall water orientation. As shown in **Figure 4a**, the order of the dipole moments of water at the interface along the *z*-direction of the mica surface is: $\text{dipole}_{z\ \text{H-mica}} < \text{dipole}_{z\ \text{Cs-mica}} < \text{dipole}_{z\ \text{Rb-mica}} < \text{dipole}_{z\ \text{Na-mica}} < \text{dipole}_{z\ \text{K-mica}}$. The same trend is observed by using the TIP4P/Ice water potential as shown in **Figure S11d**.

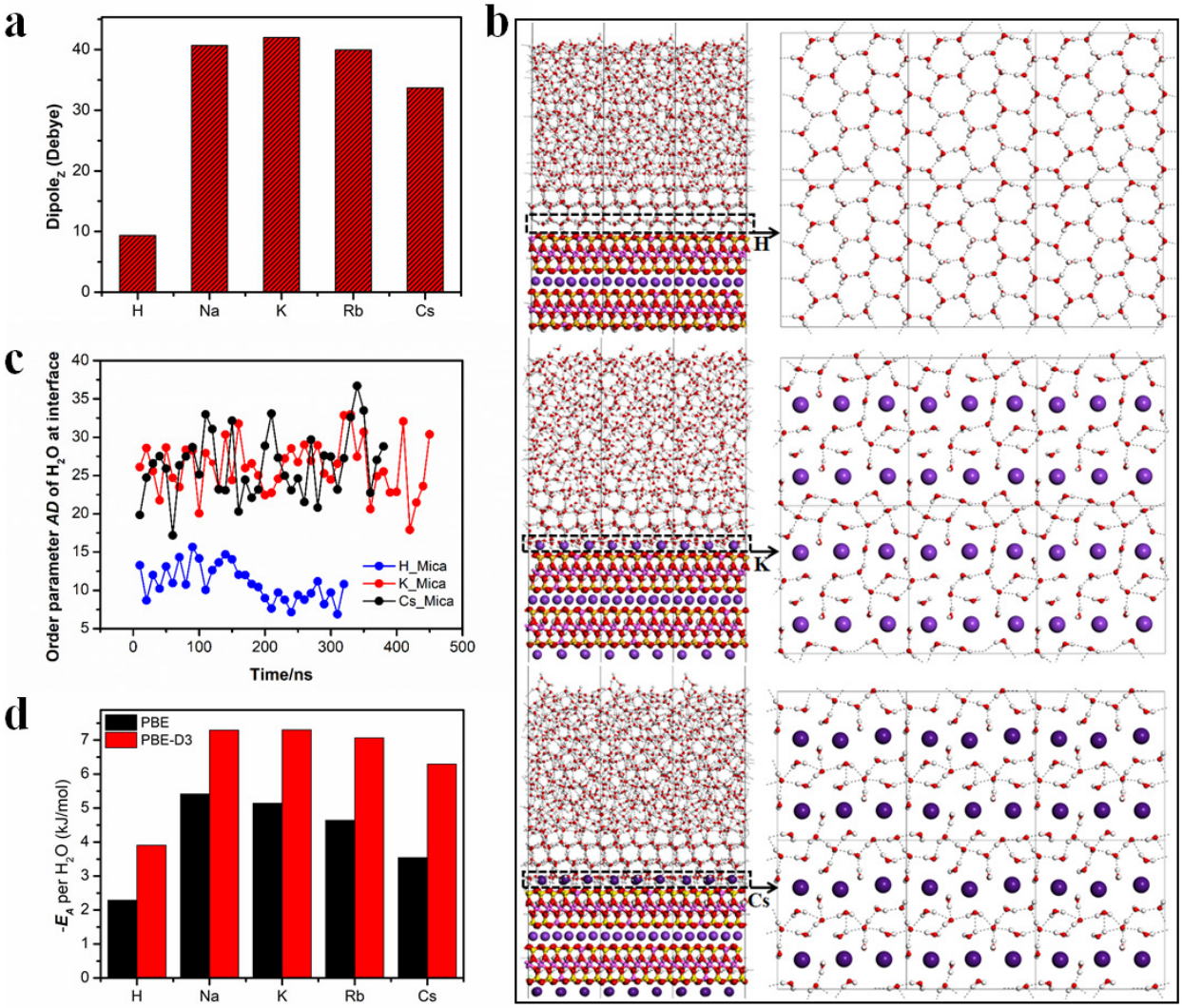

Figure 4. (**a**) Dipole projection in the z-direction of mica surfaces with various cation species. (**b**) Structure snapshots of the first water layer (right panels), right after spontaneous ice nucleation, on the H-, K-, and Cs-mica, respectively. (**c**) Computed order parameter *AD* (angle deviation) of Θ_{jik} ($\angle O_jO_iO_k$), *i.e.*, the oxygen atoms of the nearest water molecules *i*, *j* and *k* lying within 3.5 Å at the interface, with respect to the tetrahedral angle, throughout the MD simulation. Here, $AD = \langle|\Theta_{jik}-109.47|\rangle$. The smaller the *AD*, the closer to the crystalline ice on a surface the network is. (**d**) Adsorption energies E_A per H_2O between water and mica surface with various cations replacement by both PBE functional and dispersion corrected PBE functional (PBE-D3) under DFT framework.

The H-mica surface exhibits the least dipole projection in the z-direction, while the Na-/K-mica surfaces exhibit the largest dipole projection along the z-direction. The SFG measurements also suggest the smallest dipole$_z$ atop H-mica surface and obviously larger dipole$_z$ on the Na-mica surface than on the H-mica surface (**Figure 3b**); moreover, based on the freezing temperature measurements, indicating that a smaller dipole$_z$ of the interfacial water leads to a higher freezing temperature (**Figure 2b**).

To gain deeper insights into how the ion specificity induces the interfacial water to regulate the HIN on the (001) surface of mica, MD simulations were performed with the water model (TIP6P)[58]. As reported in previous studies,[60-64] TIP6P is an effective water model, particularly, allowing ice nucleation to be observed within a few hundreds of nanoseconds in the MD simulation. Here, typically, the liquid water at the interface started to freeze within 200 ns, as depicted in **Figures S12** and **S13**. The HIN of water molecules was observed to start from the second and third layers of water above the K-mica surface at about 176 ns (see **Figure S12d**), as also indicated by the second and third major peaks with doublet (see **Figure S12c**). After HIN, the ice structure continued to grow in the z-direction until the entire liquid water slab was frozen at about 450 ns (see **Figure S12e** and**12f**, and **Movie S1**). This nucleation and growth behavior is consistent with previous studies of HIN on kaolinite surface.[65,66] Similar ice nucleation and growth processes are also observed on the Na-/Rb-/Cs-mica surfaces, respectively. In contrast, on the H-mica surface (notably, H is bonded with the oxygen atoms of the mica surface in the form of OH), the HIN started from the first layer of water as shown in **Figure S13c and 13d**. Notably, the positional arrangement of the first water layer on the H-mica surface is the ice I*h* basal-like structure, as shown in **Figure 4b** (top panel), whereas the positional arrangement of the first water layer on the K-mica and Cs-mica surfaces is irregular polygons and much different with the ice I*h* basal structure (**Figure 4b** middle and bottom panels). To describe the water structure at the interface more quantitatively, we computed the order parameter *AD*, which is indicative of the mismatch between the positional arrangement of water molecules

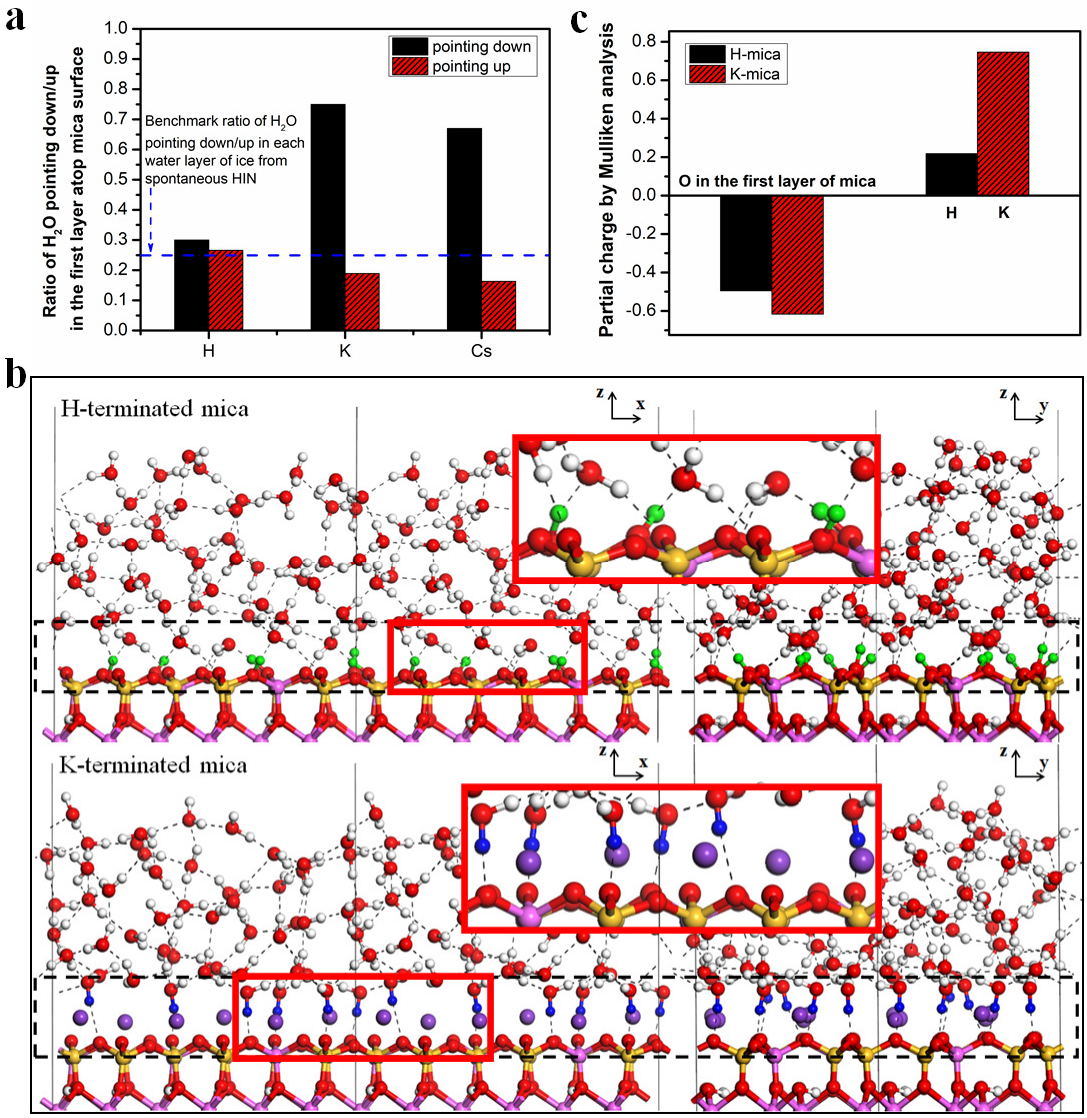

Figure 5. (**a**) Ratio of water molecules pointing down and up in the first layer of water atop mica during the spontaneous HIN processes on the H-mica, K-mica and Cs-mica surfaces. Note: the appropriate ratio of water pointing down/up in each ice layer is 25% during the spontaneous freezing processes. (**b**) Structure snapshots of water on the H-mica and the K-mica surfaces after 50 ps AIMD simulation. Green and blue balls represent the hydrogen atoms on the mica surface and the hydrogen atoms of pointing-down water molecules, respectively. Inset is the enlarged view of the red frame. (**c**) Charges carried on the oxygen atoms of the first layer of mica and charges carried on the H and K species of the H-mica and K-mica, respectively.

at the interface and that of the crystalline ice structure throughout the MD simulation (see **Figure 4c**). The *AD* of the first-layer water molecules atop the mica surface with alkali cations exhibit relatively large values compared with that of the tetrahedral H-bonded network of ice. This is due to the disordered arrangement of water molecules with irregular polygons among the gaps of the alkali cations throughout the MD simulation. On the H-mica surface, however, the *AD* values are notably smaller (**Figure 4c**). Indeed, a structural transition of the first water layer from irregular polygons to the ice I*h* basal-like structure was observed at the time of 150 – 200 ns, as shown in **Figure 4b** (top panel).

Due to the perfect lattice structure match between mica (001) and ice I*h* basal surface, the surface of mica (001) has been viewed as a template for the formation of the first layer water resembling the basal structure of ice I*h* without considering the surface cations (see **Figure S14**). If the interaction between cations and water is the same, the larger radius of the cations on the mica surface, the more likely the template effect would be broken due to the ions protruding from the mica surface, thereby lowering the HIN efficiency. It is suggested that the first water layer cannot be arranged in the form of hexagonal structures on both the K-mica and Cs-mica during the spontaneous freezing in our MD simulations (middle and bottom panels in **Figure 4b**). On the other hand, the weaker the surface adsorption energies of the water molecules are, the easier the interfacial water molecules can reorganize into the ice I*h* basal-like structures. This factor is also related to HIN efficiency, as indicated by the consistent sequence between the surface adsorption energy (**Figure 4d**) and the freezing temperature (**Figure 2b**). It is consistent with the report of Zolles *et al.* that strong ion-water interactions inhibit the ice-like structuring of water molecules in the vicinity of ions on the surface.[26] Indeed, the fact that HIN occurs more easily on the H-mica surfaces can be attributed to

both the least broken of the template effect (**Table S2**) and the lowest adsorption energy (**Figure 4d**) between the surface and interfacial water, among all cations considered in this study. Both factors are favorable for the positional arrangement of water molecules in the form of the hexagonal basal structure of ice I*h* at the interface, and for the high HIN efficiency on the H-mica surface.

To identify a relation between the distinct orientation of the interfacial water and the HIN efficiencies on the mica surfaces, the ratio of water molecules pointing down and pointing up in each water layer was evaluated and recorded during the spontaneous HIN processes. Based on the study of Shao *et al.*, the smaller the polarity of the interfacial water layer, the easier the heterogeneous water freezing on the substrate.[67] The case of interfacial water layer with the smallest polarity is 25% water molecules pointing up and 25% water molecules pointing down, which is similar to the structure of ice I*h*. As depicted in **Figures S15** and **S16,** the appropriate ratio of water molecules pointing down/up is usually 25% during the spontaneous HIN processes for water layers away from the mica surface, in which it is the smallest polarity along the normal direction of the surface. Thus, the ratio 25% of the water molecules pointing up/down in the interfacial layer is taken as the benchmark to assess the heterogeneous freezing appropriateness atop the substrate. As shown in **Figure 5a,** on the H-mica surface, the ratio of water molecules pointing down and pointing up are both around 25% in the interfacial water layer. However, on the K-mica and Cs-mica surfaces, 75% and 67% water molecules of the first layer are pointing down, while 19% and 16% water of the first layer are pointing up, respectively. The ratio of water molecules pointing down/up in the first water layer atop the K-mica and Cs-mica surfaces substantially deviates from 25%. It is this reason that water freezing on the H-mica surface is much easier than on the K-mica and Cs-mica surfaces.

Using *ab initio* molecular dynamics (AIMD) simulation, the pointing orientation of interfacial water on the H-mica and the K-mica surfaces were further confirmed (see **Movies S2** and **S3**). Indeed, water molecules on the H-mica surface present no preferential pointing orientation at the interface (**Figure 5b**), whereas O-H groups of water molecules tend to point toward the oxygen atoms of the K-mica surfaces (**Figure 5b**). To understand this behavior from the electron-transfer point of view, we computed electron density distribution and performed Mulliken charge analysis for the H-mica and the K-mica surfaces, respectively (**Figure S17**). On the K-mica surface, each oxygen atom carried more negative charges than that on the H-mica surface (**Figure 5c**) Meanwhile, each K atom atop mica surface carried more positive charges than each H atom on the mica surface. Thus, water molecules at the interface tend to point down on the K-mica surface due to the H of H_2O being attracted by more negative charges on the oxygen atoms of mica surface and the O of H_2O being attracted by the protruding K atoms with more positive charges atop mica surface.

Conclusion

We have investigated the ion-specific effect on the HIN efficiency of the mica (001) surface by measuring ice nucleation temperature $\boldsymbol{T}_{\mathrm{H}}$, ice nucleation delay time t_{D}, and SFG spectra of interfacial water, as well as by performing MD simulations. We find that the smaller dipole projection along z-direction of water at the interface tends to give higher $\boldsymbol{T}_{\mathrm{H}}$. The HIN efficiency on the mica surface also depends on the positional arrangement and the pointing orientation of the water molecules at the interface. The arrangement of interfacial water that can mimic the hexagonal ice I*h* basal structure favors the HIN, and such arrangement can be tuned by the size of the protruding cation species atop the mica surface and the surface adsorption energy. The favorable pointing orientation (25% water molecules pointing down/up in the first water layer atop mica surface) of water molecules at the interface is also crucial for the HIN, which is controlled by the surface charge distribution. Overall, the highest $\boldsymbol{T}_{\mathrm{H}}$ given by the H-mica can be attributed to a combination of several factors, namely, the formation of hexagonal ice I*h* basal-like structure of water at the interface, the weakest surface adsorption between water and H-mica surface, and the favorable pointing orientation of the interfacial water in the first water layer atop H-mica surface. In contrast, the lowest $\boldsymbol{T}_{\mathrm{H}}$ of Na-/K-mica can be attributed to the protruding cation alkali metal species atop mica surface, which prevent the formation of ice I*h* basal-like structure in the first water layer, and to the strongest surface adsorption as well as the highest deviation from the favorable pointing orientation of interfacial water resulted because of the more negative charges on the oxygen atoms of mica surface and the more positive charges on the protruding cation species atop mica surface. This comprehensive mechanistic study provides molecular-level insights into how the ion-specificity of the mica surface affects the HIN efficiency. Such insights will help to attain a better understanding of HIN on other mineral surfaces.

ASSOCIATED CONTENT

Supporting Information.
Supporting information is available free of charge via the Internet at http://pubs.acs.org."
Details of sample preparation, $\boldsymbol{T}_{\mathrm{H}}$ measurements, SFG measurements and MD simulations.

AUTHOR INFORMATION

Corresponding Author

* xzeng1@unl.edu
* bonn@mpip-mainz.mpg.de
* wangj220@iccas.ac.cn

ORCID

Shenglin Jin: 0000-0001-9427-3832
Yuan Liu: 0000-0002-8239-7704
Malte Deiseroth: 0000-0002-8810-3906
Ellen H.G. Backus: 0000-0002-6202-0280
Hui Li: 0000-0002-1725-6796
Mischa Bonn: 0000-0001-6851-8453
Jianjun Wang: 0000-0002-1704-9922

Present Addresses

†J. L.: Max Planck Institute for Polymer Research, 55128 Mainz, Germany.

Author Contributions

‡These authors contributed equally.

Funding Sources

J.J.W. acknowledges the Chinese National Nature Science Foundation (No. 51925307, 21733010 and 21703006), National Key R&D Program of China (2018YFA0208502), Key Research Program of Frontier Sciences, CAS, Grant NO. ZDBS-LYSLH031 and E.B.

acknowledges the Deutsche Forschungsgemeinschaft (DFG, German Research Foundation) - BA 5008/3 and the ERC Starting Grant (no. 336679) for support of this work.

Notes

The authors declare no competing financial interest.

ACKNOWLEDGMENT

Y. L. and X. C. Z. thank for the supporting from University of Nebraska Holland Computing Center. We also thank Leon Prädel for helping with XPS experiments. The SFG investigation was made by using the methods of Matplotlib[68] and Numpy[6957].

ABBREVIATIONS

HIN, heterogenous ice nucleation; ice nucleation temperature, T_H; ice nucleation delay time, t_D; molecular dynamics simulations, MD simulations; *ab initio* molecular dynamics simulations, AIMD simulations; Vibrational sum-frequency generation, VSFG.

REFERENCES

(1) Rosenfeld, D.; Sherwood, S.; Wood, R.; Donner, L. Climate Effects of Aerosol-Cloud Interactions. *Science* **2014**, *343*, 379.

(2) Murray, B. J.; O'Sullivan, D.; Atkinson, J. D.; Webb, M. E. Ice nucleation by particles immersed in supercooled cloud droplets. *Chem. Soc. Rev.* **2012**, *41*, 6519-6554.

(3) Kumar, A.; Marcolli, C.; Peter, T. Ice nucleation activity of silicates and aluminosilicates in pure water and aqueous solutions – Part 3: Aluminosilicates. *Atmos. Chem. Phys.* **2019**, *19*, 6059-6084.

(4) Morris, C. E.; Conen, F.; Alex Huffman, J.; Phillips, V.; Pöschl, U.; Sands, D. C. Bioprecipitation: a feedback cycle linking Earth history, ecosystem dynamics and land use through biological ice nucleators in the atmosphere. *Global Change Biology* **2014**, *20*, 341-351.

(5) Abbatt, J.; Benz, S.; Cziczo, D.; Kanji, Z.; Lohmann, U.; Mohler, O.: Solid ammonium sulfate aerosols as ice nuclei: a pathway for cirrus cloud formation. *Science* **2006**, *313*, 1770-1773.

(6) Bartels-Rausch, T. Ten things we need to know about ice and snow. *Nature* **2013**, *494*, 27.

(7) Knopf, D. A.; Alpert, P. A.; Wang, B. The Role of Organic Aerosol in Atmospheric Ice Nucleation: A Review. *ACS Earth and Space Chem.* **2018**, *2*, 168-202.

(8) Koop, T.; Luo, B.; Tsias, A.; Peter, T. Water activity as the determinant for homogeneous ice nucleation in aqueous solutions. *Nature* **2000**, *406*, 611-614.

(9) Lv, J.; Song, Y.; Jiang, L.; Wang, J. Bio-Inspired Strategies for Anti-Icing. *ACS Nano* **2014**, *8*, 3152-3169.

(10) Kumar, A.; Marcolli, C.; Luo, B.; Peter, T. Ice nucleation activity of silicates and aluminosilicates in pure water and aqueous solutions – Part 1: The K-feldspar microcline. *Atmos. Chem. Phys.* **2018**, *18*, 7057-7079.

(11) Murray, B. J.; Broadley, S. L.; Wilson, T. W.; Atkinson, J. D.; Wills, R. H. Heterogeneous freezing of water droplets containing kaolinite particles. *Atmos. Chem. Phys.* **2011**, *11*, 4191-4207.

(12) Atkinson, J. D.; Murray, B. J.; Woodhouse, M. T.; Whale, T. F.; Baustian, K. J.; Carslaw, K. S.; Dobbie, S.; O'Sullivan, D.; Malkin, T. L. The importance of feldspar for ice nucleation by mineral dust in mixed-phase clouds. *Nature* **2013**, *498*, 355.

(13) Zobrist, B.; Marcolli, C.; Peter, T.; Koop, T.: Heterogeneous Ice Nucleation in Aqueous Solutions: the Role of Water Activity. *J. Phys. Chem. A* **2008**, *112*, 3965-3975.

(14) Reischel, M. T.; Vali, G.: Freezing nucleation in aqueous electrolytes. *Tellus* **1975**, *27*, 414-427.

(15) Kiselev, A.; Bachmann, F.; Pedevilla, P.; Cox, S. J.; Leisner, T.: Active sites in heterogeneous ice nucleation—the example of K-rich feldspars, *Science* **2016**, *355*, 367-371.

(16) Murray, B. J.: Cracking the problem of ice nucleation. *Science* **2017**, *355*, 346-347.

(17) Campbell, J. M.; Meldrum, F. C.; Christenson, H. K.: Characterization of preferred crystal nucleation sites on mica surfaces. *Cryst. Growth Des.,* **2013**, *13*, 1915-1925.

(18) Connolly, P. J.; Möhler, O.; Field, P. R.; Saathoff, H.; Burgess, R.; Choularton, T.; Gallagher, M.: Studies of heterogeneous freezing by three different desert dust samples. *Atmos. Chem. Phys.,* **2009**, *9*, 2805-2824.

(19) Campbell, J. M.; Meldrum, F. C.; Christenson, H. K.: Observing the formation of ice and organic crystals in active sites. *Proc. Natl. Acad. Sci. U. S. A.* **2016**, *114*.

(20) Baustian, K. J.; Wise, M. E.; Tolbert, M. A.: Depositional ice nucleation on solid ammonium sulfate and glutaric acid particles. *Atmos. Chem. Phys.* **2010**, *10*, 2307-2317.

(21) Vergara-Temprado, J.; Murray, B. J.; Wilson, T. W.; O'Sullivan, D.; Browse, J.; Pringle, K. J.; Ardon-Dryer, K.; Bertram, A. K.; Burrows, S. M.; Ceburnis, D.; DeMott, P. J.; Mason, R. H.; O'Dowd, C. D.; Rinaldi, M.; Carslaw, K. S.: : Contribution of feldspar and marine organic aerosols to global ice nucleating particle concentrations. *Atmos. Chem. Phys.* **2017**, *17*, 3637-3658.

(22) Whale, T. F.; Holden, M. A.; Wilson, T. W.; O'Sullivan, D.; Murray, B. J.: The enhancement and suppression of immersion mode heterogeneous ice-nucleation by solutes. *Chemical Science* **2018**, *9*, 6313-6313.

(23) Hoose, C.; Möhler, O. Heterogeneous ice nucleation on atmospheric aerosols: a review of results from laboratory experiments. *Atmos. Chem. Phys.* **2012**, *12*, 9817-9854.

(24) Layton, R. G.; Harris, F. S. Nucleation of Ice on Mica. *J. Atmos. Sci.* **1963**, *20*, 142-148.

(25) Shen, J. H.; Klier, K.; Zettlemoyer, A. C. Ice Nucleation by Micas. *Journal of the Atmospheric Sciences* **1977**, *34*, 957-960.

(26) Zolles, T.; Burkart, J.; H?Usler, T.; Pummer, B.; Hitzenberger, R.; Grothe, H.: Identification of ice nucleation active sites on feldspar dust particles.. *J. Phys. Chem. A* **2015**, *119*, 2692-2700.

(27) Wagner, R.; MöHler, O.: Heterogeneous ice nucleation ability of crystalline sodium chloride dihydrate particles. *J. Geophys. Rese-Atmos.* **2013**, *118*, 4610-4622.

(28) Engelbrecht, J. P.; Moosmüller, H.; Pincock, S.; Jayanty, R. K. M.; Casuccio, G.: Technical note: Mineralogical, chemical, morphological, and optical interrelationships of mineral dust re-suspensions. *Atmos. Chem. Phys.,* **2016**, *16*, 10809-10830.

(29) Lupi, L.; Hudait, A.; Molinero, V. Heterogeneous Nucleation of Ice on Carbon Surfaces. *J. Am. Chem. Soc.* **2014**, *136*, 3156-3164.

(30) Lupi, L.; Molinero, V. Does Hydrophilicity of Carbon Particles Improve Their Ice Nucleation Ability? *J. Phys. Chem. A* **2014**, *118*, 7330-7337.

(31) Fitzner, M.; Sosso, G. C.; Cox, S. J.; Michaelides, A. The Many Faces of Heterogeneous Ice Nucleation: Interplay Between Surface Morphology and Hydrophobicity. *J. Am. Chem. Soc.* **2015**, *137*, 13658-13669.

(32) Pedevilla, P.; Fitzner, M.; Michaelides, A. What makes a good descriptor for heterogeneous ice nucleation on OH-patterned surfaces. *Phys. Rev. B* **2017**, *96*, 115441.

(33) Fitzner, M.; Sosso, G. C.; Pietrucci, F.; Pipolo, S.; Michaelides, A. Pre-critical fluctuations and what they disclose about heterogeneous crystal nucleation. *Nat. Commun.* **2017**, *8*, 2257.

(34) Bi, Y.; Cao, B.; Li, T. Enhanced heterogeneous ice nucleation by special surface geometry. *Nat. Commun.* **2017**, *8*, 15372.

(35) Sosso, G. C.; Chen, J.; Cox, S. J.; Fitzner, M.; Pedevilla, P.; Zen, A.; Michaelides, A.: Crystal Nucleation in Liquids: Open Questions and Future Challenges in Molecular Dynamics Simulations. *Chemical Reviews* **2016**, *116*, 7078-7116.

(36) Odelius, M.; Bernasconi, M.; Parrinello, M.: Two-Dimensional Ice Adsorbed on Mica Surface. *Phys. Rev. Lett.* **1997**, *78*, 2855-2858.

(37) Xu, L.; Salmeron, M. An XPS and Scanning Polarization Force Microscopy Study of the Exchange and Mobility of Surface Ions on Mica. *Langmuir* **1998**, *14*, 5841-5844.

(38) Tuladhar, A.; Chase, Z. A.; Baer, M. D.; Legg, B. A.; Tao, J.; Zhang, S.; Winkelman, A. D.; Wang, Z.; Mundy, C. J.; De Yoreo, J. J.; Wang, H.-f. Direct Observation of the Orientational Anisotropy of Buried Hydroxyl Groups inside Muscovite Mica. *J. Am. Chem. Soc.* **2019**, *141*, 2135-2142.

(39) Artsdalen, E. R. V. Complex Ions in Molten Salts. Ionic Association and Common Ion Effect. *J. Phys. Chem.* **1956**, *60*, 172-177.

(40) Qiu, Y.; Odendahl, N.; Hudait, A.; Mason, R.; Bertram, A. K.; Paesani, F.; DeMott, P. J.; Molinero, V. Ice Nucleation Efficiency of

Hydroxylated Organic Surfaces Is Controlled by Their Structural Fluctuations and Mismatch to Ice. *J. Am. Chem. Soc.* **2017**, *139*, 3052-3064.

(41) He, Z.; Xie, W. J.; Liu, Z.; Liu, G.; Wang, Z.; Gao, Y. Q.; Wang, J. Tuning ice nucleation with counterions on polyelectrolyte brush surfaces. *Sci. Adv.***2016**, *2*, e1600345.

(42) Gaines; George, L.: The ion-exchange properties of muscovite mica. *J. Phys. Chem.* **1957**, *61*, 1408-1413.

(43) Mokma, D. L.; Syers, J. K.; Jackson, M. L.: Cation Exchange Capacity and Weathering of Muscovite Macroflakes. *Soil Sci Soc. Amer. Proc.* **1970**, *34*, 146-151.

(44) Pashley, R. M.: DLVO and Hydration Forces between Mica Surfaces in Li +, Na +, K ÷, and Cs + Electrolyte Solutions: A Correlation of Double-Layer and Hydration Forces with Surface Cation Exchange Properties. *J. Colloid Interface Sci.* **1981**, *83*, 531-546.

(45) Jia, Z.; Li, X.; Zhu, C.; Yang, S.; Yang, G. Reversal of Cation-Specific Effects at the Interface of Mica and Aqueous Solutions. *J. Phys. Chem. C* **2018**, *122*, 5358-5365.

(46) Liu, K.; Wang, C.; Ma, J.; Shi, G.; Yao, X.; Fang, H.; Song, Y.; Wang, J. Janus effect of antifreeze proteins on ice nucleation. *Proc. Natl. Acad. Sci. U. S. A.* **2016**, *113*, 14739.

(47) Vali, G.: Repeatability and randomness in heterogeneous freezing nucleation. *Atmospheric Chemistry and Physics* **2008**, *8*, 5017-5031.

(48) Vali, G.: Interpretation of freezing nucleation experiments: singular and stochastic; sites and surfaces, *Atmos. Chem. Phys.* **2014**, *14*, 5271-5294.

(49) Holden, M. A.; Whale, T. F.; Tarn, M. D.; O' Sullivan, D.; Walshaw, R. D.; Murray, B. J.; Meldrum, F. C.; Christenson, H. K.: High-speed imaging of ice nucleation in water proves the existence of active sites. *Sci. Adv.***2019**, *5*, eaav4316.

(50) Herbert, R. J.; Murray, B. J.; Whale, T. F.; Dobbie, S. J.; Atkinson, J. D.: Representing time-dependent freezing behaviors in immersion mode ice nucleation. *Atmos. Chem. Phys.,* **2014**, *14*, 8501-8520.

(51) Bai, G.; Gao, D.; Liu, Z.; Zhou, X.; Wang, J.: Probing the critical nucleus size for ice formation with graphene oxide nanosheets. *Nature* **2019**, *576*, 437-441.

(52) Xue, H.; Lu, Y.; Geng, H.; Dong, B.; Wu, S.; Fan, Q.; Zhang, Z.; Li, X.; Zhou, X.; Wang, J.: Hydroxyl Groups on the Graphene Surfaces Facilitate Ice Nucleation. *J. Phys. Chem. Lett.* **2019**, *10*, 2458-2462.

(53) Lambert, A. G.; Davies, P. B.; Neivandt, D. J. Implementing the Theory of Sum Frequency Generation Vibrational Spectroscopy: A Tutorial Review. *Applied Spectroscopy Reviews* **2005**, *40*, 103-145.

(54) Abdelmonem, A.; Backus, E. H. G.; Hoffmann, N.; Sánchez, M. A.; Cyran, J. D.; Kiselev, A.; Bonn, M. Surface-charge-induced orientation of interfacial water suppresses heterogeneous ice nucleation on α-alumina (0001). *Atmos. Chem. Phys.* **2017**, *17*, 7827-7837.

(55) Glatz, B.; Sarupria, S. The surface charge distribution affects the ice nucleating efficiency of silver iodide. *J. Chem. Phys* **2016**, *145*, 211924.

(56) Abdelmonem, A.; Backus, E. H. G.; Bonn, M. Ice Nucleation at the Water–Sapphire Interface: Transient Sum-Frequency Response without Evidence for Transient Ice Phase. *J. Phys. Chem. C* **2018**, *122*, 24760-24764.

(57) Abdelmonem, A.; Lützenkirchen, J.; Leisner, T. Probing ice-nucleation processes on the molecular level using second harmonic generation spectroscopy. *Atmospheric measurement techniques discussions* **2015**, *8*, 5265-5282.

(58) Nada, H.; van der Eerden, J. P. J. M. An intermolecular potential model for the simulation of ice and water near the melting point: A six-site model of H_2O. *J. Chem. Phys* **2003**, *118*, 7401-7413.

(59) Abascal, J. L. F.; Sanz, E.; Fernández, R.; Vega, C.: A potential model for the study of ices and amorphous water: TIP4P/Ice. *J. Chem. Phys* **2005**, *122*, 234511.

(60) Vrbka, L.; Jungwirth, P. Homogeneous Freezing of Water Starts in the Subsurface. *J. Phys. Chem. B* **2006**, *110*, 18126-18129.

(61) Vatamanu, J.; Kusalik, P. G. Observation of two-step nucleation in methane hydrates. *Phys. Chem. Chem. Phys* **2010**, *12*, 15065-15072.

(62) Zielke, S. A.; Bertram, A. K.; Patey, G. N. A Molecular Mechanism of Ice Nucleation on Model AgI Surfaces. *J. Phys. Chem. B* **2015**, *119*, 9049-9055.

(63) Zielke, S. A.; Bertram, A. K.; Patey, G. N. Simulations of Ice Nucleation by Kaolinite (001) with Rigid and Flexible Surfaces. *J. Phys. Chem. B* **2016**, *120*, 1726-1734.

(64) Zielke, S. A.; Bertram, A. K.; Patey, G. N. Simulations of Ice Nucleation by Model AgI Disks and Plates. *J. Phys. Chem. B* **2016**, *120*, 2291-2299.

(65) Glatz, B.; Sarupria, S. Heterogeneous Ice Nucleation: Interplay of Surface Properties and Their Impact on Water Orientations. *Langmuir* **2018**, *34*, 1190-1198.

(66) Cox, S. J.; Raza, Z.; Kathmann, S. M.; Slater, B.; Michaelides, A. The microscopic features of heterogeneous ice nucleation may affect the macroscopic morphology of atmospheric ice crystals. *Faraday Discussions* **2013**, *167*, 389-403.

(67) Shao, M.; Zhang, C.; Qi, C.; Wang, C.; Wang, J.; Ye, F.; Zhou, X. Hydrogen polarity of interfacial water regulates heterogeneous ice nucleation. *Phys. Chem. Chem. Phys* **2020**, *22*, 258-264.

(68) Hunter, J. D. Matplotlib: A 2D Graphics Environment. *Computing in Science & Engineering* **2007**, *9*, 90-95.

(69) Oliphant, T. E. *A guide to NumPy*. Trelgol Publishing USA, 2006; Vol. 1.

For Table of Contents Only